Er-doped CdS thin films: electrical characterization

M. Rubín-Falfán[1]
Facultad de Ciencias de la Computación.
Benemérita Universidad Autónoma de Puebla, Puebla, México.

R. Lozada-Morales, J. A. Rivera-Márquez, M. R. Palomino-Merino
Facultad de Ciencias Físico Matemáticas, Posgrado en Optoelectrónica, BUAP.

O. Portillo-Moreno
Facultad de Ciencias Químicas

J. A. Dávila-Pintle
[1]Facultad de Ciencias de la Electrónica, BUAP.

O. Zelaya-Angel
Departamento de Física, Centro de Investigación y de Estudios Avanzados del IPN,
P.O. Box 14-740, México 07360, México D.F.

Cadmium sulfide thin films were prepared by chemical bath on glass substrates at 80ºC. CdS was Er-doped during the growth process by adding water-diluted $Er(NO_3)_3.3H_2O$ to the growing aqueous solution. The relative volume of the doping solution was varied in order to obtain different doping levels. Crystalline structure of CdS:Er layers was cubic zincblende for all the doped-layers prepared. The (111) interplanar distance changes in irregular way with the Er doping level. Consequently, the energy band gap (E_g) firstly increases and afterward diminishes becoming, at last, approximately constant at around E_g = 2.37 eV. For higher doping levels, in as-grown films, dark electrical conductivity (σ) values reach about 1.8 x 10^{-2} $\Omega^{-1}cm^{-1}$ at room temperature. Logarithm of σ versus 1/kT curves, where k is the Boltzmann's constant and T the absolute temperature, indicate an effective doping of CdS as a result of the Er introduction into the lattice of the material. Thermoelectric power measurements reveal an *n*-type doping with 1.1 x 10^{18} cm^{-3} as maximum carrier density.

PACS: 61.72.Vv, 73.61.Ga, 81.15.Lm
Keywords: Semiconductor; Thin film; Electrical properties; Doped layers

1. Introduction

Doping of optical materials by using rare-earth (RE) elements has been subject of interest for many years, in order to modify their physical properties for varied applications [1-3]. At present, most works in this direction is mainly developed in III-VI compound and Si semiconductors, but in the past, RE doping II-VI compounds research was so abundant because the purpose of multicolor both cathode-ray tubes and electroluminescent displays applications [4,5]. In last years, erbium has been the more employed element for doping Si, GaAs, nitrides and glasses because its luminescent properties applied to light-emitting devices fabrication,[1] nevertheless, some II-VI compounds are explored with the same purpose, with different RE elements [6,7]. In comparison with luminescent properties, electrical carrier transport in RE-doping materials is matter of little attention, however, some references can be cited in this address [8-10]. The aim of this work is to study the electrical properties of Er-doped CdS polycrystalline thin films prepared by chemical bath deposition (CBD) method. Doping was carried out chemically during the growth process, which reflect an efficient introduction of Er atoms into the semiconductor without sensitive damage of the lattice. CdS is an important material for photovoltaic [11], sensors [12], optical [13], among others, devices fabrication. Positions of Er into wurtzite (W) hexagonal CdS lattice have been studied by Watts and Holton [4]. It is expected that Er^{3+}in zincblende (ZB) cubic CdS lattice enters into Cd^{2+} sites, in such a way that *n*-type CdS layers can be obtained. Experimental results show majority negative carriers in the CdS films which allowed us to reach conductivity values up to 1.8 x 10^{-2} $\Omega^{-1}cm^{-1}$ at room temperature (RT), with a carrier density of 1.1 x 10^{18} cm^{-3}. This finding can be important for high efficiency solar cells design based in CdS/CdTe heterojunctions.

2. Experimental Details

Polycrystalline CdS thin films preparation on glass substrates at 80 ± 1 °C by CBD method has been previously reported by us [14]. The following solutions were used in the CdS:Er layers growth: $CdCl_2$ (0.02M), KOH (0.05M), NH_4NO_3 (1.5M), $SC(NH_2)_2$ (0.2M), and $Er(NO_3)_3$ $.3H_2O$ (0.5M). The total solution (100 ml) for growing CdS was completed with relative volumes (V_r) of Er-chemical agent solution since 1.0 % until 9%, in steps of 1% (1 ml), in order to obtain nine different doping levels. Growing time was 45 min for the all film depositions. The samples were named ErA-0 for undoped

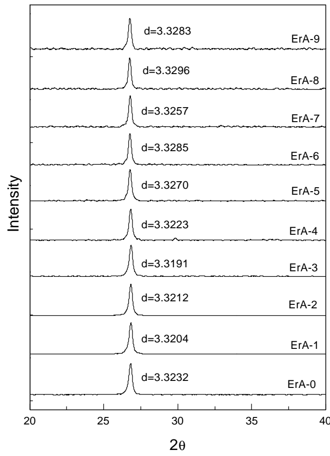

Figure 1. X ray diffraction of samples. The only visible peak is the one corresponding to (111) planes of zincblende phase. Here, *d* represents the (111) interplanar distance.

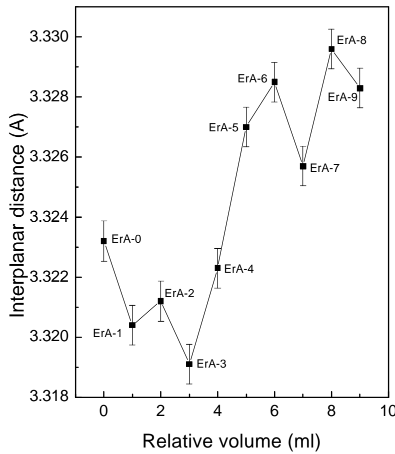

Figure 2. (111) interplanar distance (*d*) as a function of the relative volume (V_r) of doping solution for the ten samples studied.

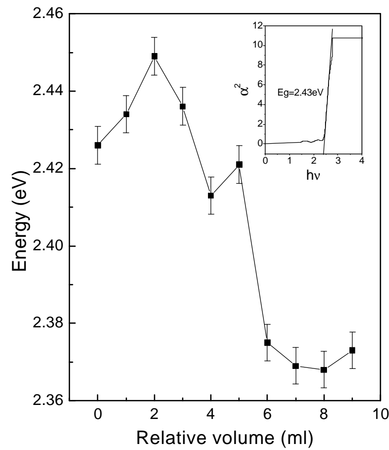

Figure 3. Band gap energy (E_g) of the CdS:Er layers plotted against the relative volume (V_r) of doping solution. The inset displays the how extrapolated straight line intercepts the photon energy (hν) axis to determine E_g

sample, and ErA-1 to ErA-9 for the other doped nine samples. Thickness of layers was in the range 200 ± 10 nm, as determined by utilizing a Dektak II profilometer. Structural characterization was carried out by means of a Siemens D5000 diffractometer, using the CuK_α line. Optical absorption spectra allowed us to calculate the forbidden energy band gap (E_g), by utilizing the α^2 versus hν plot; here α is the optical absorption coefficient and hν the photon energy. Dark sheet conductivity (σ) on fresh samples was measured in vacuum as a function of temperature (T) in the interval 100–500 K, and the sign and concentration of carriers were achieved through thermoelectric power measurements. Auger spectroscopy was used for determination of stoichiometry of layers, which indicated that the [Cd/S] ratio was in the range 1.09 – 1.02. Er concentration was found to be lower than 0.5 %at in all the samples.

3. Results and discussion

Diffractograms of doped samples display the cubic zincblende (ZB) crystalline structure for the ten different CdS:Er layers studied. Fig. 1 exhibits the (111) peak position in the 2θ axis, denoting that (111) is the preferred orientation of layers. High resolution of XRD patterns only shows very small diffraction peaks, besides the (111) one, corresponding to ZB crystalline structure. The 2θ-position variation of the maximum of the (111) peak in the spectra can be observed, which is caused uniquely by the Er introduction into the CdS lattice. The incorporation of Er^{3+}(solubility) is easier in Cd-chalcogenides than in Zn-chalcogenides, because the cation-size [4] (ionic radii, Cd^{2+}: 0.95Å, Zn^{2+}: 0.74Å, Er^{3+}: 0.89Å, S^{2-}: 1.84Å). The smaller radium of ionized Er alters the (111) interplanar distance (*d*), that gives place to distortion of the ZB-CdS lattice. Er^{3+} in cubic CdTe enters substitutionally in Cd sites [4] and in octahedral symmetric interstitial positions [15]. We assume that Er^{3+} occurs only substitutionally in ZB-CdS for low V_r, and substitutionally and interstitially for high V_r values. Figure 2 illustrates the variation of *d* with V_r, firstly, *d* decreases due to Er^{3+} in substitutive sites, afterward *d* increases owing to interstitial Er. Finally, *d* value saturates for Vr ≥ 8%. The value of *d* in the ErA-0 sample (3.3223 Å) is shorter than that reported for bulk CdS (3.3599 Å), which can be due to the polycrystalline character of CdS-films and the amorphous nature of the substrate. From optical absorption coefficient measurements the E_g-values were calculated. The inset of Fig. 3 outlines a typical α^2 vs. hν plot, the intercept of the extrapolated straight line with hν axis equals E_g. In this way, all the E_g-values were calculated and plotted against V_r, as illustrated in Fig. 3. Accordingly with Vegard's law, the E_g vs. V_r functional dependence resembles the inverse behavior of *d* vs. V_r in Fig. 2. E_g reaches a maximum value (2.45 ± 0.01 eV) at V_r = 2.0%, and a minimum value (2.37 ± 0.01 eV) for V_r ≥ 6.0%.

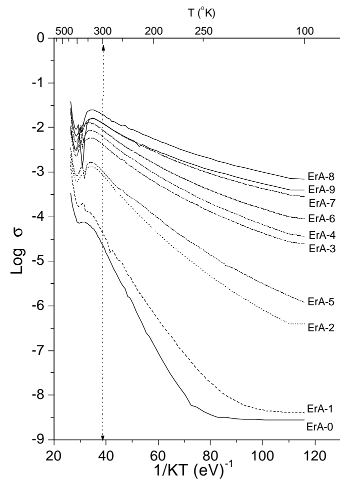

Figure 4. Dark sheet conductivity versus 1/kT for the all CdS:Er studied. T is the absolute temperature and k is the Boltzmann's constant. The vertical straight line indicates the room temperature position.

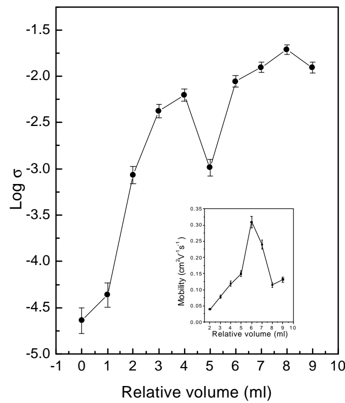

Figure 5. The logarithm of σ as a function the relative volume (V_r) of the doping solution. Measurements were carried out at room temperature. The inset exhibits the mobility versus V_r plot.

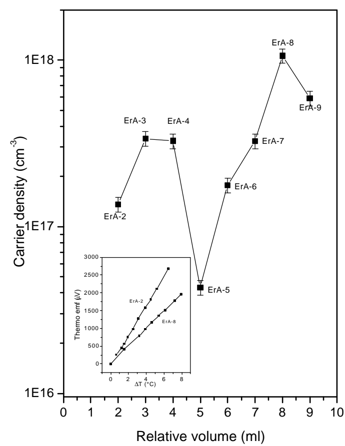

Figure 6. Carrier density of electrons plotted against V_r. The inset illustrates the experimental points followed by the thermo-electromotive force in function of the gradient ΔT of temperature applied.

Dark sheet conductivity versus inverse temperature (1/kT, where k is the Boltzmann's constant) in the range 100 – 500 K is depicted in Fig. 4 for fresh samples. In general, σ increases if V_r increases too. From the slope of the linear part of the lineshape of the Er_0 graph, an activation energy (E_a) of 0.26 ± 0.01 eV was calculated.

An E_a = 0.25 eV value in CdS was already reported by Woods and Nicholas [16] and assigned by them to Cd-excess. CdS-CBD films normally grow with a slight excess of Cd, as pointed out above in our case, then it is plausible to associate the level at 0.26 eV to this characteristic. The variation of E_a to lower values when V_r augments partially comes from E_g-values decreasing, and partially because an effective doping of CdS. The vertical dashed line in Fig. 4 points out σ values at RT. It is important to remark that as grown films were not undergone to post-thermal annealing in any ambient before σ versus T experiments. Figure 5 displays log σ vs V_r plot at RT. For $V_r > 2\%$, the behavior of σ with V_r reflects the E_g versus V_r dependence which confirms that substitutive Er^{3+} is the main source of electrons in the conduction band at RT. At around 1/kT = 32 $(eV)^{-1}$ (T = 365 K), in Fig. 4, σ reaches a relative maximum value, followed by an also relative minimum at about 1/kT = 28 $(eV)^{-1}$ (T = 415 K). Afterward, the intrinsic conductivity initiates, that is characterized by a slope in the curves of 1.19 ± 0.03 eV, i.e., ≅ $E_g/2$, where E_g = 2.41 ± 0.04 eV. The depression in the curves at T ~ 415 K, has been identified by us as originated by the annihilation of vacancy-interstitial (V-I) pairs of Cd, when Cd ions return to their original position. V-I pairs appear when the metastable cubic ZB structure attempts to transform to the stable hexagonal wurtzite (W) structure when T rises during σ versus T measurements, but the process is inhibited by the absence of sulfur vapor in the measurement chamber, in which vacuum is done [17]. These-I Cd pairs are responsible of the bowing of σ vs 1/kT curves before the maxima [17, 18]. It is important to remark that annihilation process occurs well above of RT, at T = 365 K (93 °C), that is to say, far away from CdS/CdTe solar cells performance. The maximum value σ = 1.8 x 10^{-2} $\Omega^{-1}cm^{-1}$ at RT is reached for sample ErA-8.

By means of thermoelectric power measurements carried out at RT in samples ErA-2 to ErA-9, it was possible to identify the *n*-type nature of the doping and the carrier concentration (*n*) for these films. As a matter of fact, *p*-type CdS can not exist. Fig. 6 exhibits the dependence of n for different values of V_r. ErA-8, the more conductive layer, shows an n = 1.1 x 10^{18} cm^{-3} value. The inset in Fig. 6 illustrates two typical plots of measurements of thermo-electromotive forces (ΔV) as a function of the temperature gradient (ΔT). Thermoelectric power (α = ΔV/ΔT)) let us to calculate the carrier density of electrons *n* for the ErA-2 to ErA-9 samples. The calculation was made through the relation $\alpha = -(k/e)\{A + \ln(N_e/n)\}$ [19]. In this relation when α increases, *n* decreases. The knowledge of *n* and σ and the use of the formula $\sigma = en\mu$, enabled us to calculate the mobility (μ) at RT for the different samples studied. The

inset in Fig. 5 outlines the functional dependence of μ with V_r. Clearly, a maximum value of 0.32 $cm^2V^{-1}s^{-1}$ for V_r = 6% is reached. Small values of μ (~ 0.1 $cm^2V^{-1}s^{-1}$) have been reported for CdS:In polycrystalline films [17].

Extensive statistical work made with Auger spectroscopy on each sample was useful to determine that Er-atoms concentration into the material is lower than 0.5 %at (i.e. lower than 2.07 x 10^{20} cm^{-3}). We think the actual maximum concentration of Er introduced is slightly higher than the electrically active carrier concentration 1.1 x 10^{18} cm^{-3} measured by means of thermoelectrical power, because some Er atoms are placed interstitially in the lattice of CdS. Most of these extra Er atoms are electrically inactive probably due to the formation of complexes with vacancies of Cd and/or S, which, generally, originate deep traps.

4. Conclusions

In summary, we have found an efficient process to introduce Er^{+3} ions into the CdS lattice, reaching a maximum *n*-type electrically active concentration of 1.1 x 10^{18} cm^{-3} at RT, with a dark conductivity and mobility of 1.8 x 10^{-2} $\Omega^{-1}cm^{-1}$ and 0.32 $cm^2V^{-1}s^{-1}$, respectively; which can be useful for the started point for CdS/CdTe solar cells fabrication. Furthermore, the high weight of Er may be important for elimination of doping-material diffusion toward the interface region of the heterostructured solar cells.

Acknowledgements

The authors are grateful with Dr. B. Chao for his useful measurements of Auger spectroscopy, and also with M. Guerrero, E. Ayala-Maycotte, A. B. Soto, Z. Rivera and I. Negrete for their technical assistance. This work was partially supported by CONACyT, Mexico.

References

[1] H. Shen, J. Pamulapati, M. Taysing, M. C. Wood, R. T. Lareau, M. H. Ervin, J. D. Mackenzie, C. R. Abernathy, S. J. Pearton, F. Ren, and J. M. Zavada, Sol. Stat. Electron. **43**, 1231 (1999).

[2] T. Gregorkiewicz, D. T. X. Thao, and J. M. Langer, Appl. Phys. Lett. **75**, 4121 (1999).

[3] Q. Xiang, Y. Zhou, B. S. Ooi, Y. L. Lam, Y. C. Chan, and C. H. Kam, Thin Solid Films **370**, 243 (2000).

[4] R. K. Watts, and W. C. Colton, Phys. Rev. **173**, 417 (1968).

[5] R. Boyn, Phys. Stat. Sol. (b) **148**, 11 (1988).

[6] J. Dziesiaty, St. Müller, R. Boyn, Th. Buhrow, a. Klimakow, and J. Kreissl, J. Phys. Condens. Matter **7**, 4271 (1995)

[7] N. Georgobiani, M. B. Kotljarevsky, V. V. Kidalov, I. V. Rogozin, and U. A. Aminov, J. Cryst. Growth **214/215**, 516 (2000).

[8] G. N. Ivanova, V. A. Kasiyan, and D. D. Nedeoglo, Semicond. **29**, 324 (1995)

[9] E. I. Terukov, M. M. Kazanin, O. I. Kon'kov, V. Kh. Kudoyarova, K. V. Kougiya, Yu. A. Nikulin, and A. G. Kazanskii, Semicond. **34**, 829 (2000).

[10] S. Scalese, G. Franzò, S. Mirabella, M. Re, A. Terrasi, F. Priolo, E. Rimini, C. Spinella, and A. Carnera, J. Appl. Phys. **88**, 4091 (2000).

[11] S. Ferekides, D. Marinsky, V. Viswanathan, B. Tetaly, V. Palekis, P. Selvaraj, and D. L. Morel, Thin Solid Films **361/362**, 520 (2000).

[12] K. Miremadi, K. Colbow, and Y. Harima, Rev. Sci. Instrum. **68**, 3898 (1997).

[13] M. Kobayashi, K. Kitamura, H. Umeya, A. W. Jia, A. Yoshikawa, M. Shimotomai, Y. Kato, and K. Takahashi, J. Vac. Sci. Technol. B **18**, 1684 (2000).

[14] J. L. Martinez-Montes, G. Martinez, G. Torres-Delgado, O. Guzmán, O. Zelaya-Angel, and R. Lozada-Morales, J. Mater. Sci.: Mater. Elect. **8**, 72 (1996).

[15] R. S. Title, B. L. Crowder, and J. W. Mayo, *II-VI Semiconducting Compound,* Ed. D. G. Thomas, Benjamin Inc., New York 1967. p 1367.

[16] J. Woods, and K. H. Nicholas, Britt. J. Appl. Phys. **15**, 1361 (1964).

[17] R. Lozada-Morales, M. Rubin-Falfan, O. Zelaya-Angel, and R. Ramírez-Bon, J.Phys. Chem. Solids **59**, 1393 (1998).

[18] K. B. Ramaiah, J. Mater. Sci: Mater. Elect. **10**, 291 (1999).

[19] R. H. Bube, in *Photoconductivity of Solids*, R. E. Krieger Pub. Co., New York 1978, p. a)211, b)187.